

# Early Star Formation, Nucleosynthesis, and Chemical Evolution in Proto-Galactic Clouds

Lamya Saleh

*Department of Physics & Astronomy,  
Northwestern University, Evanston, IL 60208  
email: l-saleh@northwestern.edu*

Timothy C. Beers

*Department of Physics & Astronomy and JINA: Joint Institute for Nuclear Astrophysics,  
Michigan State University, E. Lansing, MI 48824  
email: beers@pa.msu.edu*

Grant J. Mathews

*Center for Astrophysics, Department of Physics,  
University of Notre Dame, Notre Dame, IN 46556  
email: gmathews@nd.edu  
(Dated: October 22, 2018)*

We present numerical simulations to describe the nucleosynthesis and evolution of pre-Galactic clouds in a model which is motivated by cold dark matter simulations of hierarchical galaxy formation. We adopt a SN-induced star-formation mechanism within a model that follows the evolution of chemical enrichment and energy input to the clouds by Type II and Type Ia supernovae. We utilize metallicity-dependent yields for all elements at all times, and include effects of finite stellar lifetimes. We derive the metallicity distribution functions for stars in the clouds, their age-metallicity relation, and relative elemental abundances for a number of alpha- and Fe-group elements. The stability of these clouds against destruction is discussed, and results are compared for different initial mass functions. We find that the dispersion of the metallicity distribution function observed in the outer halo is naturally reproduced by contributions from many clouds with different initial conditions. The scatter in metallicity as a function of age for these stars is very large, implying that no age-metallicity relation exists in the early stages of galaxy formation. Clouds with initial masses  $\gtrsim$  presently observed globular clusters are found to survive the first 0.1 Gyr from the onset of star formation, suggesting that such systems may have contributed to the formation of the first stars, and could have been self-enriched. More massive clouds are only stable when one assumes an initial mass function that is not biased towards massive stars, indicating that even if the first stars were formed according to a top-heavy mass function, subsequent star formation was likely to have proceeded with a present-day mass function, or happened in an episodic manner. The predicted relative abundances of some alpha- and Fe-group elements show good agreement with the observed values down to metallicities below  $[\text{Fe}/\text{H}] \sim -4$  when the iron yields are reduced relative to stellar models. The observed scatter is also reproduced for most elements including the observed bifurcation in  $[\alpha/\text{Fe}]$  for stars with low  $[\text{Fe}/\text{H}]$ . However, the predicted dispersion may be too large for some elements (particularly alpha elements) unless a limited range of progenitor masses contributing to the abundances of these elements is assumed. The contributions to the abundances from supernovae with different progenitor masses and metallicity are discussed. The results suggest that the low-mass end of SNeII was probably absent at the very lowest metallicities, and that the upper mass limit for the first stars that contributed to nucleosynthesis may be  $\lesssim 40 M_{\odot}$ .

## I. INTRODUCTION

The oldest and most metal-poor stars observed in the Galaxy are mainly identified as members of the halo population, and are believed to have formed at the earliest times in the history of the proto-Galaxy. These stars are expected to have contributed to and influenced the nature of all of the various populations observed today, through their formation processes and the dynamical interactions that followed. Thus, their chemical composition and kinematic properties can provide clues to the early epochs of Galaxy formation. Accordingly, many studies have been performed to identify trends in the chemical composition of halo stars and their connection to spatial and kinematic properties [3, 4, 6, 23, 25, 26, 32, 33, 63, 64, 78, 80, 104, 112]

A dispersion in the abundances of heavy elements, varying almost no dispersion for some alpha and iron-group elements, to more than two orders of magnitude for neutron-capture elements has been detected at very low metallicities. This has led to the suggestion that the lowest-metallicity stars were the result of mixing of the ejecta from single, or at most a few, supernovae, with a limited amount of gas in the parent clouds [7, 81, 82, 97, 112]. However,

the small dispersion observed for Mg/Fe [6] may indicate that more efficient mixing of different regions occurred for ejecta containing this element and perhaps other alpha elements as well [25, 26, 33]. The present work is important in that it establishes a baseline of the predicted dispersion of various elemental ratios in the limit of little mixing among various early star-formation regions.

In addition, several studies [22, 28, 29, 65, 67, 70, 72, 105, 106, 127] have suggested a possible duality of the halo population. The observed kinematics and ages of halo field stars suggests a hybrid formation process in which the inner halo may have formed by a coherent contraction in the manner originally suggested by [40] (see also [22, 28, 127]) while the outer halo was formed by accretion of metal- poor fragments from nearby systems (e.g., [28] and references therein).

The most favored current theory for galaxy formation is based on a hierarchical clustering scenario in which the Galaxy is assembled from cold dark matter sub-galactic halos (e.g., [102]). These proto-galactic clumps are believed to have originated from density fluctuations in the early universe that accreted primordial gas from their surroundings. Merging processes would lead to larger structures, and ultimately, the Galaxy. Cold dark matter (CDM) models are consistent with the observed kinematics of the halo of the Galaxy [28, 48] and with the suggested hybrid formation scenario, but still require intensive additional observations and testing to quantify the parameters required to produce these trends in detail.

Chemical evolution models that have treated these early stages still lack a complete picture that includes all chemical and dynamical effects. They are not yet capable of providing a comprehensive picture that reproduces the scatter in observed abundances at low metallicities. Some models in the literature [3, 4, 57, 59, 60, 73, 83, 99, 107, 136, 138] have been able to reproduce, at least partially, the inhomogeneities observed for elemental abundances through a stochastic evolution scenario. These are, however, often limited for example to the study of only a few neutron-capture elements, and/or metallicity independent yields, and/or instantaneous recycling. In the present paper we incorporate metallicity dependent stellar ejecta and finite stellar lifetimes.

The enrichment processes that took place in these first structures were influenced by the initial conditions in each cloud, e.g. the initial cloud mass. While smaller clouds are susceptible to destruction by tidal forces and energetic feedback and may experience shorter episodes of chemical evolution, larger structures may have continued to enrich the interstellar media (ISM) for longer periods of time and survived the merging process, contributing eventually to the formation of the disk.

In this work we present a simple chemical-evolution model in which we evolve pre-Galactic clouds in a scenario that incorporates the main features of hierarchical galaxy formation as suggested by cold dark matter simulations. Our model is based upon several assumptions. These are: 1) In the first zero-metallicity clouds, the first-generation stars are born as population III (Pop III), explode, and the clouds that survive are enriched by their expelled yields; 2) Star formation is induced by supernovae, mainly Type II (SNeII); 3) Each individual supernova is taken to form a shell, which expands with an average velocity and triggers star formation with an average efficiency  $\epsilon$  over a timescale  $\Delta t$ ; 4) The shells' mass is the sum of the whole SNeII gas and the swept-up surroundings, and the metallicity is given by a complete mixture of both metal contents; 5) The SN II yields are taken from the literature as metal dependent; and 6) The stellar initial mass function (IMF) can differ according to various conditions within the cloud.

These assumptions, though adequate for the phenomenology of interest here, nevertheless warrant some caveats. For example, under the first assumption, one should in principle take care of details in shell fragmentation theory of shell enrichment. In the present work this is accomplished with effective star formation rates averaged over the shell.

Although assumption 2 is an appropriate scenario for enhanced star formation, it neglects some hydrodynamic negative self-regulation. For example, the hydrodynamic expansion of a SN bubble depends on the external density. In the hydrodynamic Sedov phase [31, 100, 120] energy is lost due to expansion because the expansion velocity decreases with time, and also depends on density as  $\rho^{-1/5}$ . When the ambient density is larger at an earlier times, both radius and velocity are less, so the sweep-up of surrounding gas could be smaller than assumed here. Furthermore, if subsequent stars are formed in associations, SNeII bubbles of massive stars would be expected to overlap and to form a so-called super bubble. This means that the shells' total surface is smaller, and the amount of swept-up gas is reduced.

In our model all of these details are absorbed into simple average properties of the clouds and shells. Nevertheless, these assumptions are adequate to describe the bulk of the observations, as we shall see. In particular, we incorporate the stochastic nature by which the initial conditions including total mass, and metallicity must have been distributed among the different clouds according to a hierarchical clustering scenario. This random nature is further extended during the early stages of evolution by the dependence of the chemical yields produced in SN events on the initial mass and metallicity of their progenitors. Therefore, we consider clouds of different initial masses and form stars according to four different IMFs. We also consider *metallicity-dependent* chemical yields of a number of iron group and alpha elements allowing for the products of SN events to change with time.

Assumption 4 is another very crucial assumption, since it strongly enters the metallicity results. The interstellar medium of galaxies includes a hot metal-rich gas phase that also carries these elements and could evaporate them

from the clouds. Hence, this assumption is relevant for element abundances and the timescale of their enrichment. Indeed, dwarf galaxies may require inefficient mixing of supernova ejecta with the ISM to achieve the observed low oxygen abundances and other low effective yields. We note, however, that although the full yields of SNeII may not be instantaneously incorporated and homogeneously mixed into the cool gas, in our model this loss of SN mixing efficiency can be compensated for by an increase in the star formation efficiency. Even though an increased star formation efficiency will imply more supernovae and more star formation, recall that to first order, (closed box, instantaneous recycling) the enrichment of elemental abundances only depends upon the fraction of remaining gas and not on the detailed star formation rate. Hence, for our purposes an efficient mixing of the supernova ejecta is nearly equivalent to inefficient mixing and a faster star formation rate. It is thus an adequate working hypothesis. We return to this point below.

The specific form for SN-induced star formation in our model is based upon that proposed by [138]. That is, star formation is triggered by SN events, and the material from which the next generation of stars forms is the result of complete mixing of the SN ejecta with the gas swept up from the ISM by the explosion. This produces low-metallicity stars with elemental abundances resembling the ejecta of high-mass SN progenitors, as suggested by the data.

We show that this simple stochastic model is capable of reproducing the observed scatter in abundances, relative to iron at low metallicity as well as the observed shift in trends at higher metallicities after the chemical products of stars mix with the ISM. The metallicity-dependent chemical yields of [141] used in this model, have been used previously in detail by [132], who showed general agreement with the observed relative abundances in the Solar neighborhood for most elements. They did not, however, attempt to apply these chemical yields to a stochastic, CDM-motivated model for the halo, and they only did their comparison for  $[\text{Fe}/\text{H}] \geq -3$ .

In the present work we test these yields with our model for several alpha and several iron-group elements down to metallicities below  $[\text{Fe}/\text{H}] \sim -4.0$ , near the present observational limit of metallicity in the Galaxy.

## II. THE MODEL

The main purpose of the present study is to explore the viability of a simple schematic hierarchical clustering paradigm for galaxy formation. In this picture, primordial fluctuations lead to the gravitational collapse of subsystems forming sub-galactic halos comprised of both baryons and dark matter. Such subsystems then merge and accrete diffuse matter to form proto-galactic halos. We follow the idealized chemical evolution of the baryon component of individual clouds, assuming all stars formed initially in proto-galactic clouds via SN-induced star formation (e.g., [138]). We utilize metallicity-dependent chemical yields and follow the evolution of several alpha- and Fe-group elements. These are compared to the observed abundances of individual stars in the halo and thick disk of the Galaxy.

Our model consists of evolving individual clouds in the mass range of  $10^5$  to  $10^8 M_\odot$ . We follow the chemical evolution of each cloud as a one-zone closed box [133]. The gas and stars are then explicitly evolved in time. We assume that all halo field stars were formed originally in these proto-Galactic clouds and were later dispersed by tidal forces. By varying the total masses and the star formation histories of these clouds, we attempt to account for the trends and scatter in elemental abundances observed in metal-poor stars of the halo and thick-disk populations.

Simulations show that as the baryonic component of these clouds cools (mostly via molecular hydrogen) they gravitate to the center of the dark-matter potential to form central cores [1, 95]. These cores are believed to form stars at their centers, the exact nature of which is still uncertain [24, 124]. We assume that each cloud starts with primordial material, and ultimately forms one massive star at its center. This Pop-III star later explodes as a SN event, triggering the formation of higher metallicity (population II) stars in its high-density shell. Subsequent star formation progresses in the shells of later SN events.

Star formation has been linked to the dynamical evolution of molecular clouds in many studies. Observations of nearby molecular clouds suggest that star formation is triggered by expanding shells driven by stellar winds and repeated SN events in galaxies [51, 143]. When these shells become unstable and fragment, they may form molecular clouds and stars [17, 41]. The conditions under which star formation is triggered due to the gravitational collapse of expanding shells has been investigated by [46] with a 3-D numerical simulation of the conditions in the ISM as the expanding shell injects its energy.

In all of these studies, stars are assumed to form out of the gas in the ISM and reflect its metal content at the time of their formation. Although this treatment of the star formation process in galactic chemical evolution models has been very successful in reproducing the general features of the chemical compositions of stars and HII regions in the solar neighborhood [79, 144]. it cannot be applied to the early stages of the Galaxy's evolution [123], as it fails to reproduce the observed abundance patterns in extremely metal-deficient stars [80, 112]. Therefore, an alternative scenario was proposed by Tsujimoto et al. [138] in which stars are born in the dense shells formed by the sweeping up of the ISM during a SN explosion. Ryu & Vishniac [113] suggest that such dense shells which form behind the radiative shock front are dynamically overstable and are broken into a few thousand fragments in which self gravity is

unimportant. Nakano [90] has suggested that some of these fragments will dynamically contract and eventually form stars. Such a SN-induced star formation scenario has been shown to fit the observed relative abundances at early times better than models where SN ejecta mix completely with all the gas in the ISM [89]. We adopt this scenario with a new set of equations consistent with our use of metallicity-dependent yields. The metallicity of each shell is calculated at the time of its formation and stored for use in subsequent generations.

This scenario leads to a difference between the abundances observed in stars and those of the ISM at the time they were formed. This differs from most Galactic chemical evolution models, in which the stellar and gas abundances are constrained to be identical. The material from which the next generation of stars forms, following a given SN explosion, is the result of the complete mixing of the SN ejecta with the gas swept up from the ISM by the explosion. This star formation scenario will produce low-metallicity stars with elemental abundances resembling that of a single high-mass supernova. Our model follows the evolution of gas in the clouds and the evolution of individual elements in the ISM. We also follow the chemical evolution of stars and derive the anticipated present-day metallicity distribution function for halo stars.

### A. The Calculation

We performed numerical solutions of the chemical-evolution equations for each cloud, deducing the evolution of gas mass,  $M_g$ , and mass of individual elements,  $M_i$ , in finite steps of time. At each time step, the equations are integrated over a grid of stellar masses, ranging from 0.09 to 40  $M_\odot$ . In the context of this model, we desire a time step,  $\Delta t$ , longer than the time required for a SN shell to form and disperse, but short enough to be sensitive to the short lifetimes of massive stars. For example, the expansion time of a SN event is of the order of 0.01 Myr [16], while the lifetime of the most massive stars included in our model is  $\sim 6$  Myrs. Since the sensitivity to the lifetimes is very crucial at the earliest times, the time step was taken to be  $\sim 1$  Myr up to the point when the least-massive SNe would have contributed ( $\sim 20$  Myrs). Thereafter,  $\Delta t$  was given a larger value of 25 Myrs.

We take into consideration the main sequence lifetimes of these stars, relaxing the instantaneous recycling approximation. This is of fundamental importance when dealing with timescales as short as the halo formation time, and when treating intermediate-mass elements, which receive significant contributions from progenitor stars with lifetimes comparable to the halo formation time. We adopt the mass-dependent lifetimes used by [132], i.e. the lifetimes of [118] were used for stars less massive than 11  $M_\odot$ , while the lifetimes given by the stellar evolution calculations of [140] were adopted for more massive stars

For a given cloud, when the first shell forms at  $t = 0$ , the rate at which mass goes into stars in the cloud at that time is

$$\psi(t = 0) = \epsilon M_{sh}(m, 0) / \Delta t \quad , \quad (1)$$

where  $\epsilon$  is the star formation efficiency which gives the mass fraction of the shell that is used up in forming stars. It is treated as a free parameter in our model. Changing this parameter can compensate for inefficient mixing of the supernova ejecta. Its value only has an effect on the time scales, but does not significantly alter the overall trends calculated for the elemental abundances or the MDFs. This is because to first order (closed box with instantaneous recycling) the elemental abundances are only a function of the remaining gas fraction and independent of the detailed star formation rate. In the present work, the  $\epsilon$  parameter was adjusted in this model to reproduce the shift in slope of the elemental abundance ratios for three iron-group elements below  $[\text{Fe}/\text{H}] \sim -2.4$  observed by McWilliam et al. [80]. It was also made to be consistent with the observation that the age-metallicity distribution changes for extremely metal-poor stars with  $[\text{Fe}/\text{H}] < -2.4$ .  $M_{sh}(m, t)$  is the mass of the shell formed in a SN explosion at time  $t$ , with the progenitor mass being  $m$ , and is given by :

$$M_{sh}(m, t) = E_j(m, Z) + M_{sw} \quad , \quad (2)$$

where  $M_{sw}$  is the mass of the interstellar gas swept up by the expansion. Since the explosion energy of a core-collapse supernova depends only weakly on the progenitor mass [131, 141], this quantity is taken to be constant with a value of  $5 \times 10^4 M_\odot$  [112, 123, 138].  $E_j(m, Z)$  is the mass of all the ejected material from the SN with a progenitor mass  $m$  and metallicity  $Z$ . [Note that if not all of the supernova ejecta is mixed into the ISM, then this can be compensated in our model by the star-formation parameter  $\epsilon$ .] For the first SN event the metallicity  $Z$  is zero for a population III star, and  $m$  is  $m_1$ . For later generations, the metallicity of a star is calculated from the metallicity of the shell from which it was formed,  $Z_{sh}(m, t)$ . This is calculated as a function of time, and is given by:

$$Z_{sh}(m, t) = 1 - [x_{sh}^H(m, t) + x_{sh}^{He}(m, t)] \quad . \quad (3)$$

Here,  $x_{sh}^H$  and  $x_{sh}^{He}$  are the fractions of H and He in the shell, respectively, and are given by:

$$x_{sh}^H(m, t) = [y^H(m, t) + x_{gas}^H(t)M_{sw}]/M_{sh}(m, t) \quad , \quad (4)$$

$$x_{sh}^{He}(m, t) = [y^{He}(m, t) + x_{gas}^{He}(t)M_{sw}]/M_{sh}(m, t) \quad , \quad (5)$$

where  $y^H$  and  $y^{He}$  are the mass of ejected H and He, respectively, from the explosion. We will refer to these quantities as the ‘‘yields’’. They are metallicity dependent and therefore are functions of time. The quantities  $x_{gas}^H$  and  $x_{gas}^{He}$  are the fractions of H and He in the interstellar gas at the time of formation of the shell  $t$ , respectively. This fraction is given for any element  $x_{gas}^i$  by:

$$x_{gas}^i(t) = M_i(t)/M_g(t) \quad . \quad (6)$$

For the first explosion,  $y_i(m_1, t_1)$  is the yield of elements  $i$  from stars of mass  $m_1$  and metallicity zero. The subsequent star formation rate (SFR),  $\psi(t)$ , is derived from a sum over all shells that form at time  $t$ . It thus depends on the SFR at the time the progenitor star formed,  $\psi(t - \tau_m)$ , where  $\tau_m$  is the lifetime of the progenitor.

$$\begin{aligned} \psi(t > 0) &= \int_{max(m_t, 10)}^{m_u} \epsilon M_{sh}(m_i, 0) \left[ \frac{\phi(m)}{m} \right] \\ &\times \psi(t - \tau_m) dm \end{aligned} \quad (7)$$

where  $\phi(m)$  is the IMF, normalized such that

$$\int_{m_l}^{m_u} \phi(m) dm = 1 \quad . \quad (8)$$

The quantities  $m_u$  and  $m_l$  denote, respectively, the upper and lower mass limits for the IMF. The lower mass limit for stars that produce SN events of type-II will be taken as  $10 M_\odot$ . The quantity  $m_t$  is the mass of a star with lifetime equal to  $t$ , measured from the time of formation of the first shell. Since the ejected mass from a SN changes with the metallicity of the progenitor, the quantity  $E_j(m, Z_{sh})$  in Eq. (2), must be replaced by an average over all stars of mass  $m$  and different values of  $Z_{sh}$ , which explode at a given time  $t$ :

$$\begin{aligned} \langle M_{ej}(m, t) \rangle &= \int_{max\{m(t-\tau_m), 10\}}^{m_u} dm' \\ &\times \left[ (\phi(m')/m') m_{ej}(m, Z_{sh}(m', t - \tau_m)) \right] \quad , \end{aligned} \quad (9)$$

Here,  $m'$  is the mass of the progenitor which produces the shell from which  $m$  is formed, and  $m_{ej}(m, Z_{sh}(m', t - \tau_m))$  is the mass ejected from the star with mass  $m$  and metallicity  $Z_{sh}(m', t - \tau_m)$ . The quantity  $(t - \tau_m)$  denotes both the time of formation of a star of mass  $m$  and the death of the star  $m'$ .

The same applies for the yields of individual elements,  $y_i$

$$\begin{aligned} \langle y_i(m, t) \rangle &= \int_{max\{m(t-\tau_m), 10\}}^{m_u} dm' u \left[ \phi(m')/m' \right] \\ &\times y_i^{ej}(m, Z_{sh}(m', t - \tau_m)) \quad . \end{aligned} \quad (10)$$

and  $y_i^{ej}(m, Z_{sh}(m', t - \tau_m))$  is the mass of the element  $i$  ejected from the star with progenitor mass  $m$  and metallicity  $Z_{sh}(m', t - \tau_m)$ .

The change in gas mass with time is then given by:

$$\begin{aligned} \frac{dM_g}{dt} &= -\psi(t) + \int_{max(m_t, m_l)}^{m_u} dm [\phi(m)/m] \\ &\times M_{ej}(m, t) \psi(t - \tau_m) \quad . \end{aligned} \quad (11)$$

The first term in this equation is the SFR, equal to the amount of gas going into forming stars at time  $t$ . It is derived from Eq. (7). The second term accounts for the enrichment process by all stars whose life ends at time  $t$ , including the whole possible range from  $m_t$  to  $m_u$ . The change in the mass of element  $i$  in the gas is given by:

$$\begin{aligned} \frac{dM_i}{dt} = & - \int_{\max(m_t, 10)}^{m_u} dm [\phi(m)/m] \\ & \times \epsilon M_{sh}(m, t) x_i(m, t) \psi(t - \tau_m) \\ + & \int_{\max(m_t, m_i)}^{m_u} dm [\phi(m)/m] \\ & \times y_i(m, t) \psi(t - \tau_m) . \end{aligned} \quad (12)$$

The first term in this equation gives the rate at which element  $i$  is incorporated into stars at time  $t$ , whereas the second term represents the rate at which it is being added to the ISM by stars. By substituting Eqs. (7)-(9) into equations (10) and (11), this set of integro-differential equations is solved numerically. An auto-regressive computation of the star formation rate and the metallicity of each shell that forms was employed, and previous values were substituted in equations (7) - (11) at each time step. At every time step, the metallicities of all shells formed are calculated and stored for use at later times. Each shell is recorded and the age-metallicity relation is constructed. The evolution of the metal content in both the gas and the stars are followed as a function of time.

## B. Metallicity Dependent Chemical Yields

### 1. SNII Yields

In this model we have utilized the stellar yields calculated by [141] for high-mass stars. These are more-or-less consistent with the yields of [103]. Our study is therefore complementary to the models of [3, 4] who made a similar stochastic study, but relied upon the yields of [131] and [94]. We use finely spaced mass and metallicity grids in our simulation, and linearly interpolate the yields in both dimensions. The yields of every SN event are mass- and metallicity-dependent, and the metallicities are calculated for all stars at the time of their formation and stored for use at later times. Ref. [141] included stars with progenitor masses ranging from 11 to 40  $M_\odot$ , and metallicities from zero to solar, and calculated yields for elements from H to Zn. This permits better limits to be set on Galactic chemical evolution models, and enables comparisons between the results of simulations and the empirical data from high-resolution spectral measurements in stars.

The uncertainties associated with the use of such supernova yields have been critically summarized in [3, 4]. In particular, the synthesized yields can be sensitive to various aspects of both the stellar nucleosynthesis models and the supernova explosion mechanism and energy released. As a result one needs to be cautious in inferring quantitative conclusions regarding detailed elemental abundances. Nevertheless, qualitative trends in elemental ratios can be studied. By exploring the trends based upon independent models utilizing different independently derived yields it is at least hoped that the present study will help to clarify the underlying issues in early Galactic chemical evolution. In this sense it is important to compare the present study with that of [3, 4].

It is useful to consider some of the differences between our yields and those employed by [3, 4]. While the yields presented by [141] cover stars up to 40  $M_\odot$ , other studies, such as Thielemann, Nomoto & Hashimoto (1996) obtain yields for stars up to 70  $M_\odot$ . Although the fate of stars more massive than 40  $M_\odot$  is still uncertain, recent studies have suggested that metal-free stars with masses between 35-100  $M_\odot$  collapse into black holes, while stars with masses between 10-35  $M_\odot$  can explode as SNe-II, and contribute to the enrichment process [52, 53]. In addition, including such massive stars will have very little effect on the results of a chemical-evolution calculation when adopting a Salpeter IMF, since very few stars will form that are more massive than 40  $M_\odot$ . The metallicity dependence of the yields of some elements, such as oxygen, is very strong for such massive stars. This dependence will influence greatly their evolution at early times. Since oxygen is not included in our study, we believe that the inclusion of these massive first stars is not crucial here. Therefore, the stellar mass range encompassed by the calculations of [141] is reasonable. This is also consistent with the findings of Samland (1998).

In contrast to the stellar yields calculated by [131], in which they use a constant solar progenitor metallicity, the yields [141] have the advantage of covering the whole metallicity range from zero to solar for the progenitor stars. Although their predicted yields of heavy elements are not affected greatly by small changes in the initial metallicity of the progenitor (for  $Z/Z_\odot > 0$ ), there are large differences between the predicted yields for stars with metallicity  $Z/Z_\odot > 0$  and those for stars with  $Z/Z_\odot = 0$ . This has a significant effect on the metallicity distribution of extremely metal-poor stars, and on the stars of the next generation that will form in their shells.

Ref. [141] also emphasized that, in addition to the initial mass and metallicity, the energy of the explosion is an important parameter in determining the yields from a SN event. The energy of the explosion determines the mass cutoff between the part of the synthesized elements that will be ejected and elements in the deeper layers that will fall down onto the core after the explosion. They distinguished different models A, B, and C, for stars more massive than  $25 M_{\odot}$ . These correspond to three different values for the initial kinetic energy of the “piston” (a theoretical construct used to simulate a real explosion). The larger this energy, the more heavy elements escape from the explosion. We adopt model B, an intermediate value for the energy.

## 2. Intermediate-Mass Yields

For intermediate stellar masses we adopt the standard nucleosynthesis yields of Renzini and Voli [108]. Although other tracks are available (e.g. [103]), the tracks of [108] are sufficient for the present study, which is almost unaffected by the yields of intermediate mass stars other than through the overall evolution of metallicity. The yields of [108] are also the same as those adopted in earlier works (e.g. [132]) and so are useful for comparison of the present stochastic model with the results of that earlier continuous-star-formation model.

The [108] models included stars in the mass range of  $1 < m < 8M_{\odot}$ . They calculated the yields for two different metallicities,  $Z = 0.004$ , and  $Z = 0.02$ . In the current model, we interpolated between these two values and used  $Z = .004$  yields for lower metallicities. Intermediate-mass stars mainly eject H, He, C, and N into the ISM at the end of their lives. Thus they mainly only affect the metal/H ratio.

## 3. SNIa Yields

Intermediate-mass stars mostly end their lives as carbon-oxygen rich white dwarfs. If they are members of a binary system these dwarfs may accrete mass from the remaining member to the point where their mass exceeds the Chandrasekhar limit. At this point, the star becomes unstable, causing a thermonuclear Type-Ia SN event. For these events we use the yields calculated by [130].

The appearance of the Fe-rich material contributed by Type-Ia SN is delayed by the time required by a white dwarf to evolve to an explosion. This delay time has been estimated to be of the order of 1 Gyr [50, 78, 79, 125, 129, 145]. Therefore, these events will only have a significant effect on clouds that evolve and self-enrich on a timescale of more than 1 Gyr.

Disrupted clusters disperse and permeate the halo. The dispersed remnants can produce isolated SNeIa but should not significantly affect the cloud abundances of interest in the present study. Only SNIa events which occur within the clouds affect the present study, which can be the case for clouds that are sufficiently massive to retain their gas. Less massive structures are expected to be destroyed due to the energy input from SN of Type-II events during the first Gyr of the onset of star formation. Stars less massive than  $1 M_{\odot}$  serve in this model only as reservoirs of gas mass, since they do not evolve significantly during the considered time.

## C. The IMF

In addition to the type of mixing processes following the explosion, the enrichment of the halo depends on the type and number of SN events that took place. Therefore, the central role that the IMF plays at these early times cannot be ignored. For a SN-induced star formation model, the SFR depends on the rate of death of massive stars at a given time. In other words, the SFR today depends on the SFR at previous times. Therefore, the IMF of the first stars (perhaps more properly referred to as the First Mass Function, FMF) will affect greatly the subsequent evolution of these clouds.

In this regard it is of interest that several recent studies have suggested that Pop-III stars were probably very massive [2, 18, 20, 43, 66, 88], or may have had a very massive component (Nakamura & Umemura 2002) compared to modern stellar populations.

Although the shape of the IMF that dominated in primordial conditions is still uncertain, there is compelling circumstantial evidence pointing toward an early IMF biased towards more massive stars. This evidence includes the paucity of metal-poor stars in the Solar neighborhood [i.e. the G-dwarf problem [69, 119]], observations indicating a rapid early enrichment of the ISM by heavy elements produced in the explosions of high-mass stars [71, 86], followed by slower enrichment at later times, represented by a flat age-metallicity relation in the solar neighborhood [68]. Further evidence is found in the high abundances of heavy elements in the hot gas trapped in the potential wells

of rich clusters of galaxies. The heavy-element abundance is larger than what would be predicted by a standard present-day IMF [146] and [69] and references therein.

Moreover, several studies of the central regions of star burst galaxies have suggested that the IMF is strongly biased towards high-mass stars [38, 39, 47, 109, 121]. Observations of nearby ellipticals show that  $[\text{Mg}/\text{Fe}]$  increases above the solar value with increasing galaxy luminosity [36, 142] and of distant galaxies with unusually red colors or strong 4000 Å breaks [27]. These results are suggestive of an IMF that was once weighted toward massive stars, perhaps during the early merger that was the hallmark of a forming elliptical.

A top-heavy IMF during the initial stage of elliptical galaxy formation has also been proposed as a way to account for the large iron masses in galaxy clusters [42]. Recent observations of the elemental abundances of the intracluster gas point to Type II SN as the source of enrichment, providing strong support for models with a top-heavy IMF during the formation of elliptical galaxies [71].

In addition, the elemental abundances observed in halo stars suggest that they were made out of gas enriched only by SNeII [93, 97, 112, 138]. Finally, recent theoretical calculations [88] of star formation in extremely metal-deficient clouds suggests that, in such conditions, the mass function is peaked at the high mass end (10-100  $M_{\odot}$ ) and is deficient in sub-solar mass stars.

The Salpeter power-law IMF represents the stellar distribution in the solar neighborhood very well down to 1  $M_{\odot}$ . At lower masses the form of the function is not clear due to the difficulty of obtaining a mass-luminosity relation for such faint stars. However, it is believed that it must decline rapidly and flatten below 0.1  $M_{\odot}$  in order to explain the paucity of observed brown dwarfs compared to the predictions [11, 44, 66, 69].

Empirical studies of the IMF have been conducted recently in different environments including clusters and associations in the Galaxy and the Magellanic Clouds [55, 56, 75, 139]. Although all of these studies support a Salpeter IMF with a slope in the neighborhood of  $\sim 1.35$  for stars more massive than a solar mass, some different slopes have been suggested [75, 116]. A top-heavy IMF for the first stars has also been suggested by a number of authors (e.g., [19, 69]). Two functional forms were proposed in [69].

$$\frac{dN}{d \log m} \propto (1 + m/m_l)^{-1.35} \quad , \quad (13)$$

and

$$\frac{dN}{d \log m} \propto m^{-1.35} \exp \{-m_l/m\} \quad . \quad (14)$$

These both approach the power law with a Salpeter slope at high masses and fall off at the low-mass end.

Eq. 13 falls off asymptotically to a slope zero at the low end. Eq. 14 has a peak at  $m = m_l/1.35$ , and falls off exponentially with increasing negative power at lower masses. The characteristic mass scale,  $m_l$ , has a value of 0.35  $M_{\odot}$  for the present-day solar neighborhood. This mass function was used by [54], who suggest that the IMF for population III stars was strongly weighted towards high masses at redshifts  $6 < z < 9$ . They infer a value for  $m_l$  of 12.2 at redshift  $z \sim 9$ , and metallicity  $[\text{Fe}/\text{H}] \lesssim -2.5$ , based on number counts of metal-poor stars from the HK survey [13, 14]. Both functions were tested in this model and compared to the simple power law. The mass scale was chosen to be a linear time dependent quantity of the form  $m_l = 13.2 - 0.9t$ . The range of the IMF is taken from 0.09 to 40  $M_{\odot}$ .

Figure 1 shows the different mass functions explored in this study. The first is the simple Salpeter function with index = 1.35. The second is a more moderate high-mass biased Salpeter-like function that shows a slower decline towards high masses than the simple function, but still steeper than the top-heavy functions of Larson. The two functions from Larson behave differently at low masses. While the first produces a fair amount of low-mass stars and declines slowly at the massive end, while the second function produces very few low-mass stars and peaks at an intermediate value before it declines exponentially.

#### D. Initial Conditions

The baryonic masses of globular clusters observed in the Galaxy range between  $10^4$  and  $10^6 M_{\odot}$ , while the minimum total mass of dwarf galaxies in the Local Group are  $\sim 2 \times 10^7 M_{\odot}$  [77]. Therefore, we choose initial total cloud masses in the range ( $10^5$ - $10^8$ )  $M_{\odot}$ . In this mass range, the clouds are sensitive to stellar feedback, both in terms of chemical enrichment or energetics. We start with gas in a single phase and uniform density, and choose the volume of each cloud such that we maintain a reasonable initial density in the clouds ( $\sim 0.25$  particles  $\text{cm}^{-3}$ ) corresponding to a baryon surface density of about 0.01  $M_{\odot} \text{pc}^{-2}$ . This condition is necessary in order to calculate the initial potential energy of the cloud, and its lifetime prior to destruction by SN energy input.

$M_{cloud} (M_{\odot})$	$m^{-1.35} (1 - e^{-m/2})m^{-1.35}$	$m^{-1.35} e^{-m/4}$	
$3 \times 10^6$	> 10 Gyr	-	-
$5 \times 10^6$	> 10 Gyr	9 Myr	8 Myr
$1 \times 10^7$	> 10 Gyr	80 Myr	12 Myr
$1 \times 10^8$	> 10 Gyr	200 Myr	90 Myr

TABLE I: Survival Times of the Clouds

The dark matter component of the clouds depends upon their mass and can be anywhere from 0 to  $\sim 3$  times the baryon mass, consistent with observations of rich galactic clusters (e.g., [86] and CDM simulations. The baryonic component of the clouds are taken to be composed initially of 77% (by mass) Hydrogen, 23% Helium, and a zero metallicity. The first massive star forms at the core and initiates subsequent events of SN-induced star formation. This method of star formation produces local inhomogeneities in the clouds as soon as the first SN event takes place. Each SN event will produce a group of stars reflecting the abundance pattern of that particular SN progenitor, since the stellar yields of a SN are different for different progenitor masses.

It has been shown [7] that mixing timescales in the early halo are sufficiently long that chemical inhomogeneities in the gas would not be erased on the timescale over which early generations of stars form. Therefore, we do not allow mixing between shells. Still, we assume instantaneous mixing of the shell material left behind after the explosion with the gas in the ISM.

Our clouds are self-enriched over a timescale of  $\sim 1$  Gyr. The timescale for the formation of the early halo is estimated to be of the order of a few Gyr [15], rather than  $10^8$  yrs as suggested by [40], although most of the processes that contributed to the formation of the earliest generations of stars will take place in the first 0.5 Gyr after the initiation of the first enrichment events.

### III. RESULTS AND DISCUSSION

#### A. Stability of the Clouds

Ignoring any tidal effects, heating and cooling, and any inhomogeneities in the gas, and taking the energy input per SN event  $E_{SN}$  to be  $10^{51}$  erg, we find that under the adopted initial conditions, clouds with total mass  $M_{tot} \lesssim 3 \times 10^6 M_{\odot}$  (baryon mass  $M_{baryon} = M_{tot}/(1 + M_{DM}/M_{baryon})$ ) do not survive the first SN explosion, since their total gravitational potential energy is less than  $E_{SN}$ . This zeroth order approximation implies that clouds as light as  $\lesssim 7 \times 10^5 M_{\odot}$  could survive depending upon the dark matter content. For more massive clouds, the survival time depends on the SFR chosen and on the form of the IMF. This crude estimated limit also assumes negligible  $PdV$  work by the expanding gas since we assume that the external pressure from the cloud is small and fragmentation of the shell may reduce this kind of energy loss.

The initial density has a large effect on the stability of a cloud, and we must keep in mind that star-forming regions become cooler and denser as time passes. As they form stars, the clouds are heated by the thermal input from massive stars. Therefore, such a simple treatment can only give a rough estimate of the fate of these clouds. Table I shows the survival times of our model clouds against destruction, as a function of initial mass, for three different mass functions.

It is clear from the table that the fate of clouds which survive the first explosion varies greatly depending on the type of the IMF chosen. The Salpeter function produces very few massive stars, which allows enrichment to continue in all clouds more massive than  $5 \times 10^6 M_{\odot}$  for times longer than 10 Gyr. At the same time, clouds as massive as  $10^8 M_{\odot}$  do not survive more than  $\sim 0.1$  Gyr with a top-heavy IMF. This leads to the suggestion that even if the first stars were formed according to a top-heavy IMF, subsequent star formation must have involved an IMF similar to the present day mass function [9].

This result is in agreement with recent studies concerning the type of IMF expected to govern mass formation in the past and present [54, 69, 87, 88, 137]. In Ref. [69] suggested the existence of a mass scale in the star-formation process which varies with cloud conditions such as pressure and temperature, and therefore is time dependent. If the temperature in star-forming clouds was higher at early times, this will have the effect of increasing the mass scale and the relative number of low-mass stars formed at early times will decrease. He also suggested another possible form of IMF with a universal power-law form at large masses, but that departs from this power law below a characteristic time-dependent mass scale.

Empirical evidence has supported this picture, with a power-law form of the IMF down to one Solar mass (see §2.3). Recent chemical evolution models have tested the time varying IMF in the Galaxy as a solution to the G-dwarf problem (e.g., [74]. These authors have found that an IMF with two slopes, and a time-dependent shape at the

low mass end, is required to reproduce constraints other than the G-dwarf problem. They also show that such a function is still not able to reproduce the properties of the Galactic disk and suggested the inclusion of radial flows to reproduce the observed trends. Invoking different slopes of the IMF in order to explain the G-dwarf problem is a long-standing way to address this problem which has fallen out of favor (see above). More recently, however, dynamical effects, both of the infall of low-metallicity gas, and radial outflow of hot metal-rich gas (e.g., [114] have provided a somewhat more plausible mechanism to produce these effects. Nevertheless, the question still remains as to whether the mass function has varied with time and needs to be addressed further by including dynamical effects in the models of galactic evolution. For the purposes of the present study a simple time-dependent IMF is adequate.

Our model is consistent with the clouds being the environment out of which the globular clusters first formed. It is necessary for the efficiency  $\epsilon$  of star formation be very high for globular cluster formation. The gravitational binding of the star cluster that is formed must therefore dominate, because gas expulsion did not lead to the cluster's disruption. The cloud mass which survives disruption ( $\sim 7 \times 10^5 M_\odot$ ) is consistent with observed globular cluster masses, particularly if some evaporation has occurred to the present time. In our model, sufficiently massive GCs could have been self enriched. Indeed, a recent more detailed model by [101] for the formation of globular-cluster systems suggests that they were indeed self enriched.

Alternatively, globular clusters could have been formed initially in more massive stable systems such as dwarf galaxies. The homogeneous chemical composition of stars within most globular clusters seems to suggest that they formed out of gas that was already pre-enriched and well mixed inside structures that were more stable against destruction. The globular cluster population of the halo might then be explained as the result of accretion events during tidal interactions with other galaxies. This was suggested by [5] and [69].

As mentioned previously, our calculation of the lowest mass of a cloud that can survive the first SN event is very simplistic and is not meant to be a basis for understanding globular cluster formation and survival. Among other things, our model ignores hydrodynamical effects and inhomogeneities/fragmentation in the gas. More precise understanding of these first clouds is required before definite conclusions can be made about the formation of globular cluster systems.

In clouds that do survive SN explosions, star formation halts when there is not enough gas to form the shells that trigger the process. Hence, the SN-induced star formation method used here is capable of self regulation. If these clouds are allowed to accrete gas from any other source, another sequence of star formation is possible. This is consistent with the observations that suggest that the Sgr dwarf galaxy has had an episodic star formation history [84].

## B. Stellar Abundances and Metallicities

The self-enriching fragments of gas, in which the first stars are formed, will eventually be destroyed either by internal stellar feedback or by external effects such as tidal forces. Star formation is then halted. The extremely metal-poor stars left behind contribute to the halo field population, and contain information about the nucleosynthesis of elements in zero-metallicity stars, their IMF, and the environment in which the first clouds formed. Thus, we next compare the results of our calculation to the observed abundance trends in the Galaxy.

## C. Metallicities and Ages of Stars

The metallicities of stars are calculated in this model from the metallicities of the shells formed by SN events. (In this study, metallicity always refers to the value of  $[\text{Fe}/\text{H}]$ .) The first star that explodes is a metal-free Pop-III star. Its ejecta depends on its initial mass. The ejecta will mix with a given amount of primordial gas to determine the metal composition of second-generation stars. Figure 2 shows the metallicities produced in shells of different progenitors as a function of time. They are shown for four different progenitor masses: 13, 20, 30 and 40  $M_\odot$ . The metallicities produced at early times range from  $[\text{Fe}/\text{H}] \sim -2.5$  to values well below  $[\text{Fe}/\text{H}] \sim -4$  for the most massive progenitors of  $\sim 40 M_\odot$ . This implies that it might be possible to form Pop-II stars with  $[\text{Fe}/\text{H}] < -4$ . This is in agreement with the existence of low-mass star with extremely iron abundance (e.g.  $[\text{Fe}/\text{H}] = -5.3$  [30]).

Figure 2 also shows that SNeII produce shells that do not exceed an initial metallicity of  $[\text{Fe}/\text{H}] \lesssim -2.5$ . Note, that this upper limit of  $[\text{Fe}/\text{H}] \lesssim -2.5$  is based upon a complete mixing of the supernova ejecta into the shell. If this mixing were less efficient, for example by the loss of ejecta from the cloud in a jet, this limiting metallicity would be appropriately reduced. The fact that this limit is the value of metallicity at which Ref. [80] observed a shift in the slope for relative abundances vs. metallicity suggests that mixing of ejecta with the shell must be rather efficient. This value of metallicity separates two different stages of chemical evolution, the era of inhomogeneous composition dominated by SNeII, followed by a stage of rapid iron enrichment by type-Ia SN. As long as the mixing of the ejecta

is efficient, this also supports the idea that only a few SN events are required to raise the heavy-element abundances from zero to the values observed in the most metal-poor stars in the halo.

In Figure 3 we show the age-metallicity relation for stars in a cloud of initially primordial gas, and assuming a Salpeter mass function. This cloud was allowed to evolve up to 10 Gyr. The ejecta of type-Ia SN contributed after a delay time of 1 Gyr. Each point on the figure represents a shell that formed stars. The mean value of  $[\text{Fe}/\text{H}]$  increases with time, as expected. Stars of the same age show a dispersion in metallicities that increases for older stars. This is not predicted by a simple one-zone model that assumes complete mixing, and is a result of the star formation mechanism applied in this model, i.e. that stars form out of the material ejected in Type-II SN events. This will allow for a variety of chemical composition depending on the progenitor masses and metallicities.

This large scatter, decreasing with time, can be explained by the fact that stars are formed only during SN events. Therefore, stars are the result of the mixing of SN ejecta with a limited amount of gas. This produces stars of different elemental ratios even if they form at the same time, since the SN ejecta are dependent on both the initial mass and metallicity of the progenitor.

The most-massive SNe would contribute first and reflect their yields in the first Pop-II stars to appear, then at later times the products of the less-massive SN are expected to appear with different elemental ratios [141]. This does not necessarily mean that the first and most massive SNe will produce the lowest metallicity Pop-II stars. It is the lowest mass SNeII that produce shells as low in metallicity as  $[\text{Fe}/\text{H}] \sim -4$ , while 20 to 30  $M_{\odot}$  progenitors produce higher metallicity shells.

When enough time has passed for the ISM to mix on a large scale, the elemental ratios are expected to reflect an average of the ejecta of SN events of differing masses, including those of type-Ia. The steep rise at early times reflects the dominance of SN individual events with different effective yields, and a high efficiency for the enrichment of the metal-poor ISM. The gradual increase at later times is due to the slower enrichment process involving a well-mixed ISM. It is clear from the scatter in the figure that a simple age-metallicity relation probably does not exist at early times.

#### D. The Metallicity Distribution Function (MDF)

Ref. [22] compared the kinematics and chemical properties of metal-poor stars as a function of distance from the Galactic plane. They found that stars closer to the plane exhibit a slightly more metal-rich mean abundance,  $\langle[\text{Fe}/\text{H}]\rangle \approx -1.7$ , while those farther from the plane have  $\langle[\text{Fe}/\text{H}]\rangle \approx -2.0$ . This was also confirmed by [12]. This was postulated to result from the existence of two discrete components in the halo. The flattened, inner component was probably formed in a manner resembling the [40] model, while the more spherical, outer halo had a large contribution from nearby smaller systems similar to the Sagittarius dwarf galaxy or other proto-dwarf galaxies. This is in agreement with the hierarchical CDM model citeKauffman93. The halo MDF is therefore generally believed to be the result of combining the distribution functions of individual proto-dwarf galaxies accreted by the Galaxy (cf. [34, 117] and references therein).

Although many recent studies of the formation of the halo are supportive of such a scenario [21, 35, 37], when comparing the observed features of present-day dwarf galaxies to those of the (presumably) accreted stars and clusters, one finds inconsistencies. The so-called *satellite catastrophe* [76, 85] the *angular momentum catastrophe* [92], and comparisons of abundances and ages in large and dwarf galaxies, lead to the conclusion that present day dwarfs are probably not the major building blocks of large galaxies like the Milky Way [8, 62, 122, 135]. This is not necessarily in disagreement with hierarchical galaxy formation theories. One can still argue that the satellite systems that built large galaxies may have been different from present-day dwarfs, and that these systems are not visible today [128]. For a more detailed discussion, see [134].

The observed MDF of metal-poor stars in the Galaxy shows a relatively broad peak with a maximum at  $[\text{Fe}/\text{H}] \sim -1.6$ , and a smooth tail extending to values of  $[\text{Fe}/\text{H}] \lesssim -3$ . In contrast, the metallicity distribution of disk stars shows a more localized peak with a sharp cutoff [110, 111]. This suggests that the environment in which the disk formed was probably more uniform than that which formed the halo stars.

A number of authors (e.g., [28, 96] have suggested that there might be a "bump" in the halo MDF at lower metallicities. A feature not expected from the simple model, this bump might be suggestive of non-uniform enrichment at early times. In this picture, pre-Galactic clouds are assumed to be the building blocks of the halo. Therefore, their metallicity distributions will contribute to the total MDF of the halo. The MDF is expected to vary from cloud to cloud depending on the initial conditions and the duration of chemical enrichment.

As a crude approximation to the effect of an expected range of combined MDF's we made a simple study of the MDF's of four different clouds, each evolved with a different IMF. We did this under the assumption that all these clouds eventually disperse and contribute to the field of the halo. The time evolution of the MDF was followed up

to the time of each cloud’s destruction. In the case of the Salpeter mass function, for example, the evolution was followed up to 5 Gyr and was found to saturate at 1 Gyr.

Figure 4 shows the results for the four clouds, where the type of mass function chosen for each cloud is shown on the figure (all MDFs were normalized to unity). The panels shown in Figure 4 indicate that the chemical enrichment in the first cloud, with a simple power-law mass function, is much slower than in the other three clouds with mass functions biased toward massive stars. Therefore the timescales chosen for this figure are different, since the enrichment is slower and with the short timescales used in the other three panels, one would not be able to see the full evolution picture in this cloud.

At the beginning all of the clouds show a dispersion, with the majority of stars at metallicities below  $[\text{Fe}/\text{H}] = -5$ . This describes the first stars that form from the shells of the most massive progenitors with  $m > 35 M_{\odot}$ . This could also be concluded from Figure 2, which shows that only these massive stars form such low-metallicity shells.

As time goes on, less-massive stars will contribute shells in the metallicity range  $-3 \leq [\text{Fe}/\text{H}] \leq -2.5$ . These produce a rapid increase in the numbers of stars in this metallicity range. Moreover, these stars should greatly outnumber the first stars formed from higher-mass explosions. As soon as stars with  $m \leq 20 M_{\odot}$  start to contribute, shells with metallicities down to  $[\text{Fe}/\text{H}] \sim -4.5$  form and a dispersion is seen once again. This dispersion eventually diminishes as the inhomogeneities start to disappear and the stars become more metal rich. The final stage shows a peak at a different value of metallicity for each cloud. This illustrates the different enrichment produced by the different mass functions.

The first cloud, with a simple mass function, achieves a peak at  $[\text{Fe}/\text{H}] = -2.7$ , a value consistent with the calculations of [112] and [91] for the expected metallicity of Pop-II stars formed in the shell of a typical SN expelled into primordial gas. The other clouds produce higher metallicity peaks, corresponding to the larger number of massive stars that they produce. These peaks have the values  $[\text{Fe}/\text{H}] = -2.6, -2.5, \text{ and } -2.2$ , respectively. The latter corresponds to the fourth mass function shown in Figure 1, which produces the largest number of massive stars.

In Figure 5 we illustrate the sum of the final stages of all four clouds. This produces a broader distribution extending from about  $[\text{Fe}/\text{H}] = -3.2$  to about  $[\text{Fe}/\text{H}] = -2.2$  and peaked at a value of  $[\text{Fe}/\text{H}] = -2.6$ . The MDF observed in the halo shows a yet broader distribution, than that indicated on Figure 5. This is probably due to the large number of different systems that contributed to it, and a higher value for the maximum mass indicating contributions from systems that may have produced stars from pre-enriched gas.

## IV. RELATIVE ELEMENTAL ABUNDANCES

### A. The Observed Trends in Halo Stars

Very metal-poor halo stars show a great diversity in their absolute elemental abundances and can show considerable scatter (up to a factor of 100) in the observed abundances of heavy elements relative to Fe [25, 49, 80, 82, 98, 110, 112, 126]. At higher metallicities the scatter gradually decreases until this ratio terminates at a value that corresponds to an average over the IMF of the element to iron ratios of the stellar yields.

McWilliam et al. [80] detected a shift in the slope of the abundances of the elements Al, Mn, Co, Cr, Sr, and Ba relative to Fe below  $[\text{Fe}/\text{H}] \sim -2.5$ . They suggested that this unusual chemical composition must have originated from the fact that supernova yields changed with time, or in other words, are metallicity dependent. These results were confirmed later in [112] who also showed that the scatter in the abundance ratios increases with decreasing  $[\text{Fe}/\text{H}]$ .

Under the assumption of efficient mixing of the supernova ejecta with the clouds, these observations support the idea that the most metal-poor stars exhibit the ejecta of very small numbers of supernovae. The metallicity-dependent yields used in our present model, together with the unique method of SN-induced star formation, are capable of explaining these trends. The observed relative abundances in the halo are fully reproduced with this model for several elements. These results are summarized and discussed in the following sections.

### B. Overview of Model Predictions

To obtain a picture of the early elemental abundance evolution, simulations were run for 5 Gyr using a massive cloud ( $10^7 M_{\odot}$ ), and a Salpeter initial mass function. After 1 Gyr, SN of type-Ia were allowed to contribute their ejecta. The elemental abundances were calculated and recorded for every shell that forms during the simulation. The model produces a small number of stars at very low metallicities,  $[\text{Fe}/\text{H}] < -3$ , showing a considerable spread in  $[X/\text{Fe}]$  ratios, ranging from less than 0.5 dex in the case of Ca and Ti to as much as 1 dex for Mg [33] [see however [6] who obtain almost no dispersion for Mg]. The observed scatter of the abundances for model stars is given by the spread in

metallicities of the SN models. Therefore, the large scatter in the abundance ratios observed in low-metallicity stars is inherently reproduced by the stochastic nature of this model.

Local inhomogeneities start to disappear at  $-3.0 < [\text{Fe}/\text{H}] < -2.5$ , corresponding to  $\sim 0.1$  Gyr from the onset of star formation. At this stage most of the massive SNe have contributed, and their ejecta have already mixed with the gas in the ISM. This metallicity range marks the end of the early phase and the beginning of the transition to the well-mixed phase. At this stage, the gas becomes more metal-rich. Hence, newly formed stars will no longer exhibit abundance patterns of a single SN, but rather an average over the IMF of the supernovae that contributed to the enrichment of the local ISM. These values resemble the predictions of a simple one-zone model in which stars are assumed to form out of the well mixed gas in the ISM. The spread in the relative abundances decreases gradually, reflecting the ongoing mixing process as more SNe pollute the ISM, and the values of  $[\text{X}/\text{Fe}]$  approach the solar value.

### C. $[\alpha/\text{Fe}]$

Figure 6 shows  $[\alpha/\text{Fe}]$  vs.  $[\text{Fe}/\text{H}]$  for several alpha elements calculated by a straightforward application of the model (small dots). These are compared with two sets of observational data, Ryan et al. [112] (triangles) and Norris et al. [98] (circles). The observed values show an over-abundance relative to solar, and a scatter that is significant at all values of  $[\text{Fe}/\text{H}]$ , larger at the lowest abundances. There is also a peculiar trend in the data whereby some stars which appear to have increasing  $[\alpha/\text{Fe}]$  with decreasing  $[\text{Fe}/\text{H}]$  which shows up as an extension in the data. This behavior is apparent in the abundances of Mg, Ca, and Si. On the other hand, Ti shows a scatter that is almost constant over the metallicity range.

The over-abundance in alpha elements relative to iron compared to the Sun can be understood as the result of the dominance of SNeII at the time, since they are believed to be the major production sites for alpha elements. This also indicates that the corresponding stars formed within the first Gyr of the onset of significant star formation. After 1 Gyr, type-Ia SN events are expected to shift the trends with large amounts of Fe. Therefore, the ratios decline gradually toward solar metallicities. The so-called plateau for  $[\alpha/\text{Fe}]$  ratios at low metallicities has been shown [6, 10, 26, 33] to have less dispersion (at least for some elements) than previously thought [81, 98, 112]. This dispersion can set strong limits on the nature of the first SNe, and the nature of the enrichment process when compared to the predictions of chemical evolution models.

More recent studies of the abundances of metal-poor stars show similar trends in general [25, 45, 58]. In addition, all three studies report the detection of stars with low alpha-element abundances relative to iron, in contrast to the majority of metal-poor stars. To explain these observations, they suggest that these stars probably experienced enrichment from type Ia SN events [58], owe their origins to lower mass stellar systems with slower enrichment histories [25], or were formed in the Galaxy but at times of nonuniform mixing where a mass function that produces less high mass stars (which are responsible for producing Mg as less massive SNII produce the heavier alpha elements) would be responsible for the low-alpha stars. This is an interesting phenomena that needs to be included in a complete picture for the chemical evolution of the Galaxy, once enough data is available, since it does have the potential to set limits on the type and number of SN events that took place in the environment from which these stars formed.

A number of groups [6, 25, 26, 33] have analyzed a sample of extremely metal-poor stars, down to low metallicities,  $[\text{Fe}/\text{H}] \geq -3.0$ . They find that the scatter in the abundance ratios  $[\text{X}/\text{Fe}]$ , is surprisingly small, even at the lowest metallicities, compared to what is expected from a stochastic early evolution. They suggest several ideas to reduce the scatter predicted by chemical evolution models, including effective mixing to maintain the chemical homogeneity in the clouds, limiting the mass range of the IMF, introducing a first generation of very massive stars ( $> 100 M_{\odot}$ ), and relaxing the closed-box approximation.

As seen in Figure 6, our most naive model reproduces some of the general observational trends for alpha elements relative to iron. However, the model tends to overestimate the scatter for alpha elements, and exhibits overall lower values than expected for  $[\text{X}/\text{Fe}]$  ratios. The model points also may turn down too rapidly with metallicity for  $[\text{Fe}/\text{H}] > -3$ . This suggests an over production of Fe. This is most evident in Mg and Ti, which show mean values of  $[\text{X}/\text{Fe}]$  that are 0.5 dex lower than the data all the way down to the lowest metallicities. Ca and Si show better agreement below  $[\text{Fe}/\text{H}] < -3$ , but also decline and reach subsolar values as  $[\text{Fe}/\text{H}]$  increases. The suggestion by [132] of reducing the amount of Fe produced by massive stars seems to be required, especially in the cases of elements Mg and Ti. This indicates the uncertainty in the Fe yields, which is representative of Fe-group elements in general, and will be discussed in the next section. The overproduction of Fe can also be attributed to the contributions of SNIa. A delay time longer than 1 Gyr may be required. Although this is a possibility, it still seems more likely that the Fe yields from SNeII are responsible, since the apparent underproduction of alpha elements seen in our calculation is not seen for Fe group elements as well.

Figure 7 shows the results of our model when the Fe yield is reduced by a factor of 2. The agreement between the data and the calculation in this case is much improved. We even produce the bifurcation of trends, e.g. in  $[\text{Mg}/\text{Fe}]$

and  $[\text{Si}/\text{Fe}]$  there are two trends in the data. One is a flattening at  $[\text{X}/\text{Fe}] \sim 0.5$ , and another a linear increase in  $[\text{X}/\text{Fe}]$  with decreasing metallicity. In our model, these two trends are an artifact of which type of star produced the first supernova. The metallicity-dependent yields of Ca reproduce the values of  $[\text{Ca}/\text{Fe}]$  and the scatter at low metallicities very well, and show a flattening with decreasing metallicity. This was also observed in the samples analyzed by [25, 26, 33]. In [25] it was further suggested that the scatter in  $[\text{Si}/\text{Fe}]$  ratios at low metallicity is due to uncertainties in the observational techniques used for this element. Our results for the alpha element Ti shows lower values than the data and rather little dispersion. This is consistent with the most recent observations (e.g. [26, 33]). However, as for any element, the less abundant it is, the more uncertain is its production rate, as calculated from supernova models. This is surely the case with Ti.

Previous studies (e.g., [4]) have found that such stochastic models tend to predict too much scatter (e.g. for O and Mg) and fail to reproduce the trends of other elements. Our model is also based upon a stochastic picture and also can overestimate the scatter in Mg compared to the most recent observations unless a modification in the yields is adopted as in [4]. This will be discussed in more detail in §4.5.

#### D. [Fe-peak / Fe]

For Fe-peak elements, the element abundance ratios relative to iron are close to solar down to a metallicity  $[\text{Fe}/\text{H}] \gtrsim -2.5$ . That is, except for Mn, which is underabundant in all halo stars. Below this ( $[\text{Fe}/\text{H}] \lesssim -2.5$ ), the behavior changes [80, 81, 98, 112]. Both Cr/Fe and Mn/Fe decrease to sub-solar values, Co/Fe increases to super-solar values, and Ni maintains an average value slightly above solar. The scatter increases towards lower metallicities. The correlation seen between Cr/Fe and Mn/Fe ratios (both increasing with increasing metallicity), was speculated by Carretta et al. [25] to be an indication of the absence of very massive stars ( $m \geq 100 M_{\odot}$ ), since they argue that these stars would under-produce nuclei with odd nuclear charge. Therefore,  $[\text{Mn}/\text{Fe}]$  would decrease with metallicity while  $[\text{Cr}/\text{Fe}]$  would remain approximately constant. They suggested an explanation for the trends of these ratios decreasing with decreasing  $[\text{Fe}/\text{H}]$  as due to variation in mass cuts in SNeII events as a function of progenitor mass. The observed trends can be reproduced if the mass cut is smaller for larger progenitor masses, which presumably were more common at lower metallicities.

Figure 8 shows the calculated values of relative abundances for Cr, Co, Mn and Ni. The observed ratios of Mn and Ni are reproduced well by the metallicity-dependent yields of [141] in this model. Cr, on the other hand, does not seem to produce satisfactory results. The stars produced at very low metallicity show a small over-abundance relative to solar, contrary to the observed under-abundance. The excess in Co/Fe was produced fairly well with the metallicity-dependent yields below  $[\text{Fe}/\text{H}] = -2.5$  if the contributions from SN more massive than  $40 M_{\odot}$  are excluded (see section 4.5). This behavior of Co at the lowest metallicities has not been produced by any previous models, and no known stellar yields were able to predict it even by modifications in explosion parameters of SN-II models (e.g. [89]).

Our calculations raise the questions as to how well the nucleosynthesis of massive stars is understood, especially for progenitors of low metallicity. The dependence of the yields of these elements on the position of the mass cut and degree of mixing for material ejected from SNe is one of the primary sources of large errors in calculated abundance yields. Mn and Cr are produced mainly during explosive Si burning, and therefore have a complicated dependence on the progenitor mass. Efforts to understand the abundance trends of iron-peak elements, which are formed close to the mass cut, have focused on the possible alpha-rich freeze-out [80], the location of the mass cut, and the dependence of yields on the star mass, metallicity, and neutron excess [89]. Our model predicts a scatter in the ratios for Fe-group elements that is larger at very low metallicities than the observed values. Mostly this large scatter is contributed from the products of SNe more massive than  $35 M_{\odot}$ . This may suggest that these stars do not contribute and end their lives as a black hole (see §4.5). This could also be attributed to the several approximations made in the model, especially the exclusion of any overlap or mixing among SN shells.

#### E. Contributions from Different Supernovae

The ejecta of the most massive stars are expected to dominate the earliest phases of the chemical evolution of each cloud. These stars produce values of  $[\text{Fe}/\text{H}] < -2.5$  in their shells. According to [141], at zero metallicity, the most massive stars ( $35 M_{\odot} < M < 40 M_{\odot}$ ) produce metallicities lower than that observed, while the lowest observed metallicities of  $[\text{Fe}/\text{H}] \sim -4$  are produced by progenitors of masses less than  $20 M_{\odot}$ . These various behaviors of SNe with different progenitor masses is responsible for the dispersion in metal abundances at low metallicities. Studying the dispersion in the relative abundances of elements in the halo will allow for constraints to be set on chemical

evolution models. It can help us understand the nature of the first SNe, and the inhomogeneous enrichment processes that took place. It also constrains the nature of the IMF and star formation rates at the corresponding times.

Figures 9 to 12 show the contributions to the elemental abundances by different progenitor masses down to metallicities of  $[\text{Fe}/\text{H}] = -5$  and up to  $-2.5$ . This range represents the early stages of chemical evolution in the Galaxy for which our model is applicable. Once  $[\text{Fe}/\text{H}] > -2.5$ , the contributions from SNIa pollute the ISM and the contributions from SN of Type II become less dominant. For these figures, we have run the simulation allowing only a range of progenitor masses to contribute its ejecta. The mass ranges are shown on the figures. The same is shown for Fe-group elements in Figures 13 to 16.

The main feature that can be seen in all eight figures is that the progenitors responsible for producing extremely low metallicities in the Galaxy are either more massive than  $35 M_{\odot}$  or less massive than  $20 M_{\odot}$ . Figure 2 shows that these extremely low-metal stars are only produced at the earliest times, and therefore, are probably the products of Pop-III stars. Also, it is the high-mass progenitors  $m \gtrsim 40 M_{\odot}$  that produce shells with metallicities way below  $[\text{Fe}/\text{H}] = -5$ , while the progenitors with  $m \lesssim 20 M_{\odot}$  can only produce shells with metallicities down to  $[\text{Fe}/\text{H}] \gtrsim -4$ . Therefore, the fact that the ejecta of the high mass progenitors is missing at low metallicities, while the current belief is that they have been available in the halo from the beginning, can definitely be attributed to a lack of data. And while the search for lower metallicity stars continues, this will remain an open question.

A scarcity of extremely low-metal stars in the Galaxy may suggest that the first stars that formed in pre-Galactic clouds formed out of pre-enriched gas, and that there are no Pop-III stars in the Galaxy. Or that stars more massive than  $35 M_{\odot}$  do not contribute their ejecta, and instead, end their lives as black holes.

The missing ejecta of SN events with progenitors less massive than  $20 M_{\odot}$  in the data, at low metallicities, may be suggestive of the fact that such stars are not produced at the earliest times, in support of the theory that a top-heavy IMF dominated star formation in pre-Galactic clouds. However, this interpretation may be obscured if SNeII remnants do not expand as single bubbles, but accumulate and amalgamate so that they cover larger mass ranges. Another feature in the figures supporting this idea is that for several elements (Mg, Cr, Co, Ni and Mn), the calculated relative abundances that lie outside the observed ranges at metallicities  $[\text{Fe}/\text{H}] > -4$  are either contributed partially (as in the cases of Ni, Cr, and Co), or totally (as in the cases of Mg and Mn) by stars less massive than  $25 M_{\odot}$ . This is suggestive of the fact that SNe that contributed before  $[\text{Fe}/\text{H}] \sim -2.5$  were all massive. In the cases of the elements Ni, Co and Cr, we can also see contributions outside the observed ranges of relative abundances coming from stars more massive than  $35 M_{\odot}$ . This also may imply that these stars do not contribute as SNeII. When these SNe at the low-mass and high-mass end are not allowed to contribute at the earliest stages, the model fits very well the observational data [6, 25, 26] which report less scatter than previous studies.

Again we need to keep in mind here that the nucleosynthesis calculations of these elements are still not certain enough to allow us to build accurate conclusions regarding their production. Therefore, we do see here that there is a great need to study these early stages of chemical evolution in more detail in order to be able to set limits on the details of the production of these elements.

The calculated values from the high-mass progenitors do not fit the observed values for Co even at higher metallicities, while the rest of the mass range down to  $10 M_{\odot}$  reproduces the observations very well. This result for the low-mass end is in contrast to what is found for the other elements Mg, Ti, Cr, and Mn. In these cases, the low-mass progenitors produce values of the relative abundances out of the range of the data. This may be suggestive of the fact that the first stars were massive and that the SNe that contributed before  $[\text{Fe}/\text{H}] \sim -2.5$  were all massive. The alpha-element enhancement observed for stars with  $[\text{Fe}/\text{H}] < -2.5$  is indicative of a high-mass IMF in the first Gyr of the Galaxy's formation. After this time, as type-Ia SN contribute their Fe ejecta, at  $[\text{Fe}/\text{H}] \sim -2.5$ , the alpha-element ratios go down to solar values.

## V. SUMMARY AND CONCLUSION

We developed a CDM-motivated model to simulate the stochastic early chemical evolution of proto-Galactic clouds in the halo. This model is based upon a SN-induced star-formation mechanism which keeps track of the chemical enrichment and energy input to the clouds by Type II and Type Ia supernovae. An important feature of this model is the implementation of metallicity-dependent yields for all elements at all times, and the inclusion of finite stellar lifetimes. These were found to have important effects on the metallicity distribution functions for stars in the clouds, their age-metallicity relation, and relative elemental abundances for of alpha- and Fe-group elements.

A crude estimate of the stability of these clouds against destruction was considered, and results depend upon the dark matter content, the external pressure, the energy input from supernovae, and the initial mass function for low-metallicity stars. Most clouds with initial masses similar to presently observed globular clusters were found to survive disruption from the onset of star formation, suggesting that these systems could possibly have been responsible for the formation of the first stars, and could provide an environment for the self-enrichment of globular clusters. However,

such clouds are only stable when one assumes an initial mass function that is not too biased towards massive stars, indicating that even if the first stars were formed according to a top-heavy mass function, subsequent star formation may need to have proceeded with a present-day mass function, or happened in an episodic manner.

An important conclusion of this study is that the dispersion of the metallicity distribution function observed in the outer halo is naturally reproduced by contributions from many clouds with different initial conditions. The scatter in metallicity as a function of age for stars in our simulations is very large at early times, implying that no age-metallicity relation exists in the very earliest stages of galaxy formation.

Regarding observed elemental abundances, the observed scatter is reproduced fairly well for most, but not all, elements. In particular, the predicted relative abundances of alpha elements compared to iron can be made to agree with the observed values down to a metallicity below  $[\text{Fe}/\text{H}] \sim -4$ , but only if the total iron produced is reduced by a factor of two from our adopted [141] yields. Similarly, iron group elements Cr, Co, Mn, and Ni all exhibit abundance trends vs.  $[\text{Fe}/\text{H}]$  that are somewhat different than those observed. The simplest explanation for both of these phenomena within our model is to move the mass-cut for iron and iron-group elements outward in the stellar models for all stars except those with masses in the range  $25 < m < 35 M_{\odot}$ . If yields are restricted in this way a good fit to all elements can be obtained. We note, however, that though this is a simple explanation, we can not rule out that these trends could result from some of the previously noted shortcomings of the model rather than a stellar evolution effect. For example, the reduced iron and iron-group yields could perhaps equally well have been achieved by relaxing the assumption of efficient mixing of the ejecta with the cloud.

A particularly reassuring result of the present study with regard to alpha elements is that these models naturally predict the observed detailed trends. That is, these models reproduce both stars which increase in  $[\alpha/\text{Fe}]$  with decreasing  $[\text{Fe}/\text{H}]$  and stars which obtain a near constant value of  $[\alpha/\text{Fe}]$  albeit with a significant scatter. In these models, this bifurcation of the abundance distributions can be attributed to whether the initial supernovae within the clouds were massive  $m \sim 40 M_{\odot}$  progenitors or of lower mass.

The contributions to the abundances from supernovae with different progenitor masses and metallicity suggest that the low-mass end of Type-II SN was probably absent at the very lowest metallicities, and that the upper mass limit for the first stars that contributed to nucleosynthesis may be  $\lesssim 40 M_{\odot}$ .

### Acknowledgments

Work at Michigan State University supported by grants AST 95-29454, AST 00-98549, and AST 00-98508, as well as PHY 02-16783, Physics Frontier Centers/JINA: Joint Institute for Nuclear Astrophysics, awarded by the National Science Foundation. This paper represents the thesis work of L. Saleh completed at Michigan State University in partial fulfillment of the requirements for a Ph.D. degree. L. Saleh acknowledges the doctoral dissertation completion fellowship granted to her by Michigan State University through the research grants summarized above.

Work at the University of Notre Dame supported by the US Department of Energy under Nuclear Theory grant DE-FG02-95ER40934.

- 
- [1] Abel, T., Bryan, G., & Norman, M. L. 1999, in *H2 in Space*, eds. F. Combes, G. Pineaudes
  - [2] Abel, T., Bryan, G.L., & Norman, M. 2002, *Science*, 295, 93
  - [3] Argast, D., Samland, M., Gerhard, O.E., Thielemann, F.-K. 2000, *A&A*, 356, 873
  - [4] Argast, D., Samland, M., Thielemann, F.-K. & Gerhard, O.E. 2002, *A&A*, 388, 842
  - [5] Armandroff, T.E. 1993, in *Galaxy Evolution: The Milky Way perspective*, Proc. of Seminar Series held at the Observatories of the Carnegie Institution of Washington, 1992. Ed., Steven R. Majewski; (Astronomical Society of the Pacific) P. 167
  - [6] Arrone, E. Ryan, S. G., Argast, D. Norris, J. E. & Beers, T. C. 2004, *Astron. Astrophys*, **430**, 507
  - [7] Audouze, & Silk 1995, *ApJ*, 451, L49
  - [8] Baldacci, L., Clementini, G., Held, E.V., Momany, Y. 2002, in *New Horizons in Globular Cluster Astronomy*, G. Piotto, G. Meylan, G. Djorgowski, M. Rielo eds., ASP Conf. Ser. 228, 2003 p. 355
  - [9] S. K. Ballero, F. Matteucci, C. Chiappini 2006, *New Astron.*, 11, 306-324
  - [10] P. S. Barklem, N. Christlieb, T. C. Beers, V. Hill, M. S. Bessell, J. Holmberg, B. Marsteller, S. Rossi, F.-J. Zickgraf, D. Reimers 2005, *Astron. Astrophys.*, 439, 129
  - [11] Basri, G., Marcy, G. W 1997, *Star Formation Near and Far: Seventh Astrophysics Conference*. Eds. Steven S. Holt and Lee G. Mundy. Woodbury N. Y., 1997, AIP Conf. Ser. 393., p.228
  - [12] Beers, T. C., Christlieb, N. Norris, J. E., Bessell, M. S., Wilhelm, R., AllendePrieto, A. C., Yanny, B., Rockosi, C., Newberg, H. J., Rossi, S., Lee, Y. S. 2005IAUS..228..175B
  - [13] Beers, T. C., Preston, G. W. & Shectman, S. A. 1985, *AJ*, 90, 2089

- [14] \_\_\_\_\_ . 1992, AJ, 103, 1987
- [15] Bekki, K., Chiba, M. 2000, ApJ, 534, L89
- [16] Binney J. & Tremaine S. 1987, *Galactic Dynamics*, (Princeton University Press: Princeton)
- [17] Blondin, J. et al. 1988, ApJ, 500, 342.
- [18] Bromm, V., Coppi, P.S., Larson, R.B. 2002, APJ, 564, 23
- [19] Bromm, V., Ferrara, A., Coppi, P.S., Larson, R.B. 2001a, MNRAS, 328, 969
- [20] Bromm, V., Kudritzki, R. P. & Loeb, A. 2001b, ApJ, 552, 464
- [21] Brook, C.B., Kawata, D., Gibson, B.K., Flynn, C. 2003, astro-ph/0301596
- [22] Carney, B.W., Laird, J.B., Latham, D.W., & Aguilar, L.A. 1996, AJ, 112, 668
- [23] Carney, B. W., Wright, J. S., Sneden, C., Laird, J. B., Aguilar, L. A., Latham, D.W. 1997, A J, 114, 363
- [24] Carr, B. J., Bond, J. R., & Arnett, W. D. 1984, ApJ, 277, 445
- [25] Carretta, E., Gratton, R., Cohen, J.G., Beers, T.C., Christlieb, N. 2002, AJ, 124, 481
- [26] Cayrel, R. et al. 2004, A&A, 416, 1117
- [27] Charlot, S., Ferrari, F., Mathews, G. J. & Silk, J. 1993, ApJL, 419, L57
- [28] Chiba, M., & Beers, T.C. 2000, AJ, 119, 2843
- [29] Chiba, M., & Beers, T.C. 2001, ApJ, 549, 325
- [30] Christlieb, N., Bessell, M.S., Beers, T. C., Gustafsson, B., Korn, A., Barklem, P.S., Karlsson, T., Mizuno-Wiedner, M., Rossi, S. 2002, Nature, 419, 904
- [31] Chioffi, D. F., McKee, C. F. & Bertschinger, E. 1988, ApJ, 334, 252
- [32] Cohen, J.G., Christlieb, N., Beers, T.C., Gratton, R., Carretta, E. 2002, AJ, 124, 470
- [33] Cohen, J.G., C. Norbert, A. McWilliam, S. Stechman, I. Thompson, G. J. Wassweburg, I. Ivans, M. Dehn, T. Karlsson, J. Melendez 2004, ApJ, 612, 1107
- [34] Cote, P., Marzke, R.O., West, M.J., Minniti, D. 2000, ApJ, 533, 869
- [35] Cote, P., West, M.J., & Marzke, R.O. 2002, ApJ, 567, 853
- [36] Davies, R. L., Sarler, E. M. & Peletier, R. F. 1993, MNRAS, 262, 650
- [37] Dinescu, D.I., Majewski, S.R., Girard, T.M., Mendez, R.A., Sandage, A., Siegel, M.H., Kunkel, W.E., Subasavage, J.P., Ostheimer, J. 2002, ApJL, 575, L67
- [38] Doane, J. S., Mathews, W. G. 1993, ApJ, 419, 573
- [39] Doyon, R., Joseph, R. D. & Wright, G. S. 1994, ApJ, 421, 101
- [40] Eggen, O.J., Lynden-Bell, D. & Sandage, A.R. 1962, ApJ, 136, 748
- [41] Ehlerova, S., Palous, J., Theis, Ch., & Hensler, G. 1997, A&A, 328, 121
- [42] Elbaz, D., Arnaud, M. & Vangioni-Flam, E. 1995, A&A, 303, 345
- [43] Elmegreen, B.G. 2000a, AJ, 539
- [44] Elmegreen, B.G. 2000b, MNRAS, 311, L5
- [45] Fulbright, Jon P. 2002, AJ, 123, 404
- [46] Elmegreen, B.G., Palous, J., Ehlerova, S. 2002, MNRAS, 334, 693
- [47] Elmegreen, B.G. 2004, MNRAS, 354, 367
- [48] Font, A. S., Johnston, K. V., Bullock, J. S., Robertson, B. 2006, ApJ, 638, 585
- [49] Gratton, R.G., & Sneden, C. 1994, A&A, 287, 927
- [50] Greggio, L., & Renzini, A. 1983, A&A, 118, 217
- [51] Hartmann, L. 2002, ApJ, 578, 914
- [52] Heger, A., Fryer, C.L., Woosley, S., Langer, N., Hartmann, D. H. 2003, ApJ, 591, 228
- [53] Heger, A., Woosley, S., Waters, R. 2000, "The First Stars", Eds. A. Weiss, T. Abel & V. Hill, Proceedings of the MPA/ESO Workshop, Garching, Germany
- [54] Hernandez, X., & Ferrara, A. 2001, MNRAS, 324, 484
- [55] Hunter, D. A., Tolstoy, E., Lynds, R., O'Neil, E. 1997, American Astronomical Society Meeting, 191, 81.04
- [56] Hillenbrand, L. A. 1997, AJ, 113, 1733
- [57] Ishimaru, Y. & Wanajo, S. 1999, ApJL, 511, L33
- [58] Ivans, I.I., Sneden, C., James, C.R., Preston, G.W., Fulbright, J.P., Hoefflich, P.A., Carney, B.W., Wheeler, J.C. 2003, ApJ, 592, 906
- [59] Karlsson, T. and Gustafsson, B. 2005 Astron. Astrophys., 436, 879
- [60] Karlsson, T. 2005 ApJ, 439, 93
- [61] Kauffman, G., White, S.D.M., & Guiderdoni, B. 1993, MNRAS, 264, 201
- [62] Kauffman, G., Heckman, T., White, S., Charlot, S., Tremonti, C., Peng, E., Seigert, M., Brinkmann, J., Nichil, R., SubbaRao, M., York, D. 2003, MNRAS, 341, 54
- [63] King, J.R. 1997, AJ, 113, 2302
- [64] Kinman, T., Castelli, F., Cacciari, C., Bragaglia, A., Harmer, D, Valdes, F. 2000 A&A, 364, 102
- [65] Kinman, T., Suntzeff, N.B., Kraft, R.P. 1994, AJ, 108, 172
- [66] Kroupa, P. 2002, in *Modes of Star Formation*, E.Grebel, W.Brandner (eds), ASP Conf. Ser., 285, 86.
- [67] Lance, C. 1988, ApJ, 334, 927
- [68] Larson R.B. 1986, MNRAS, 218, 409
- [69] Larson R.B. 1998, MNRAS 301, 569
- [70] Lee, J.W., & Carney, B.W. 1999, AJ, 118, 1373
- [71] Loewenstein, M. & Mushotzky, R. F. 1996, ApJ, 466, 695

- [72] Majewski, S.R. 1992, ApJS, 78, 87
- [73] Malinie, G. Hartmann, D.H., Clayton, D. D. & Mathews, G.J. 1993, ApJ, 413, 633
- [74] Martinelli, A., Matteucci, F. 2000, A&A, 353, 269
- [75] Massey, P., Hunter, D. A. 1998a, ApJ, 493, 180
- [76] Mateo, M.L., 1998, ARA&A, 36, 435
- [77] Mateo, M. 2000, *The First Stars*, Proc. Of the MPA/ESO Workshop, Garching, August 1999. Achim Weiss, Tom G. Abel, Vanessa Hill (eds.), Springer.
- [78] Mathews, G.J., Bazan, G., Cowan, J.J. 1992, ApJ, 391, 719
- [79] Matteucci, F. & Greggio, L. 1986, A&A, 154, 279
- [80] McWilliam, A., Preston, G. W., Sneden, C., Searle, L. 1995, AJ, 109, 2757
- [81] McWilliam, A. 1997, ARA&A, 35, 503
- [82] McWilliam, A. 1998, AJ, 115, 1640
- [83] McWilliam, A., Searle, L. 1999, Ap&SS, 265,133
- [84] Mighell, K. J., Sarajedini, A., French, R. S. 1999, New Views of the Magellanic Clouds, IAU Symposium 190, Eds. Y.-H. Chu, N. Suntzeff, J. Hesser, & D. Bohlender., p.445
- [85] Moore, B., Ghigna, S., Governato, F., Lake, G., Quinn, T., Stadel, J., Tozzi, P. 1999, ApJ, 524, L19
- [86] Mushotzky, R. et al. 1996, ApJ, 466, 686
- [87] Nakamura F., Umemura, M. 2001, ApJ, 548, 19
- [88] Nakamura F., Umemura, M. 2002, ApJ, 569, 549
- [89] Nakamura, T., Umeda, H., Nomoto, K., Thielemann, F., Burrows, A. 1999, ApJ 517, 193
- [90] Nakano, T. 1998, ApJ, 494, 587
- [91] Nakasato, N. & Shigeeyama, T. 2000, ApJL, 541, L59
- [92] Navarro, J.F., & Steinmetz, M., 2000, ApJ, 538, 477
- [93] Nissen, P., Gustafsson, B., Edvardsson, B., & Gilmore, G. 1994, A&A, 285, 440
- [94] Nomoto, K. Iwamoto, K., Kishimoto, N. 1997, Sci., 276, 1378
- [95] Norman M. L., Abel T., Bryan G. 2000, "The First Stars", Proceedings of the MPA/ESO Workshop, Garching, Germany Eds. A. Weiss, T. Abel & V. Hill, (Springer Verlag, Heidelberg), p. 250
- [96] Norris, J.E. 1999, *The Galactic Halo*, ASP Conf. Ser., Vol. 165, p.217
- [97] Norris, J.E., Beers, T.C., Ryan S.G 2000, ApJ, 540, 456
- [98] Norris, J.E., Ryan, S.G., & Beers, T.C. 2001, ApJ, 561, 1034
- [99] Oey, M. S. 2003, MNRAS, 339, 849
- [100] Ostriker, J. P. & McKee, C. F. 1988, Rev. Mod. Phys., 60, 1
- [101] Parmentier, G. 2004, Mon. Not. R. Astron. Soc., 351, 585
- [102] Peacock, J. 1999, Proc. of the MPA- ESO Cosmology Conference, Garching, Germany, *Evolution of large scale structure : from recombination to Garching*, edited by A. J. Banday, R. K. Sheth, L. N. da Costa. Garching, Germany : European Southern Observatory, p.64
- [103] Portinari, L., Chiosi, C. & Bressan, A. 1998, A&A, 334, 505
- [104] Preston, G. W. & Sneden, C. 2000, AJ, 120, 1014
- [105] Preston, G.W., Shectman, S.A., & Beers, T.C. 1991, ApJ, 375, 121
- [106] Preston, G., Beers, T.C., & Shectman, S.A. 1994, AJ, 108, 538
- [107] Raiteri, C. M., Villata, M., Gallino, R., Busso, M., Cravanzola, A. 1999, ApJ, 518, L91
- [108] Renzini, A., & Voli, M. 1981, A&A, 94, 175
- [109] Rieke, G. H. et al. 1993, ApJ, 412, 99
- [110] Ryan, S. G., Norris, J.E. 1991a, AJ, 101, 1835
- [111] Ryan, S.G. & Norris, J.N. 1991b, AJ, 101, 1865
- [112] Ryan, S. G., Norris, J. E., & Beers, T.C. 1996, ApJ, 471, 254
- [113] Ryu, D., & Vishniac, E.T. 1987, ApJ, 313, 820
- [114] Samland M., Hensler, G., & Theis, Ch. 1997, ApJ, 476, 544
- [115] Samland, M. 1998, ApJ, 496, 155
- [116] Scalo, J. 1998, *The Stellar Initial Mass Function* (38th Herstmonceux Conference) eds. Gary Gilmore and Debbie Howell, ASP Conf. Ser., Vol. 142, p.201
- [117] Scannapieco, E., & Broadhurst, T. 2001, ApJ, 550, L39
- [118] Schaller, G., Schaerer, D., Meynet, G., & Maeder, A. 1992, A&A Sup. Ser., 96, 269
- [119] Schmidt, M. 1963, ApJ, 137, 758
- [120] Sedov, L. 1946, Prikl. Mat. Mekh., 10(2) 241
- [121] Shadmehri, M. 2004, MNRAS, 354, 375
- [122] Shetrone, M.D., Cote, P., & Sargent W.L.W. 2001, APJ, 548, 592
- [123] Shigeeyama, T. & Tsujimoto, T. 1998, ApJ, 507, L135
- [124] Silk, J. 1983, MNRAS, 205,705
- [125] Smecker, T. & Wyse, R.F.G. 1991, ApJ, 372, 448
- [126] Sneden, C., Cowan, J. J., Burris, D. L., Truran, J. W. 1998, ApJ,496, 235
- [127] Sommer-Larsen J., Beers, T.C., Flynn, C., Wilhelm, R., & Christensen P.R. 1997, ApJ, 481, 775
- [128] Steinmetz, M. 2003, A&SS, 284, 325 (2003)
- [129] Tantalo, R., & Chiosi, C. 2002, A&A 338, 396

FIG. 1: The different mass functions used in the model,  $\phi_1 = m^{-1.35}$ ,  $\phi_2 = (1 - e^{-m/2})m^{-1.35}$ ,  $\phi_3 = (1 + m/ml)^{-1.35}$ ,  $\phi_4 = m^{-1.35} e^{-ml/m}$ .

FIG. 2: Metallicity enrichment vs. time in the first 2 Gyr for shells containing progenitor stars of various masses. The progenitors shown have masses 13, 20, 30 and 40  $M_{\odot}$ .

- [130] Thielemann, F.-K., Nomoto, K., Yokoi, K. 1986, A&A, 158,17
- [131] Thielemann, F.-K., Nomoto, K., & Hashimoto, M. 1996, ApJ, 460,408
- [132] Timmes, F.X., Woosley, S.E., & Weaver, T.A. 1995, ApJS, 98, 617
- [133] Tinsley, B.M. 1980, *Fundamentals of Cosmic Physics*, 5, 287
- [134] Tosi, M. 2003, Ap&SS, 284, 623
- [135] Tolstoy, E., Venn, K.A., Shetrone, M., Primas, F., Hill, V., Kaufer, A., Szeifert, T. 2003, AJ, 125, 707
- [136] Travaglio, C., Burkert, A., Galli, D. 2000, *The Galactic Halo : From Globular Clusters to Field Stars*, Proceedings of the 35th Liege International Astrophysics Colloquium, Eds. A. Noels, P. Magain, D. Caro, E. Jehin, G. Parmentier, and A. A. Thoul. Liege, Belgium : Institut d'Astrophysique et de Geophysique, p.135
- [137] Tumlinson, J. 2006 Mon. Not. R. Astron. Soc., in press
- [138] Tsujimoto, T., Shigeyama, T., & Yoshii, Y. 1999, ApJ, 519, L63
- [139] von Hippel, T. , Gilmore, G., Tanvir, N., Robinson, D., Jones, D. H. P. 1996, AJ, 112, 192
- [140] Weaver T.A., Woosley, S.E. 1994, ApJ, in prep.
- [141] Woosley, S.E. & Weaver, T.A. 1995, ApJS, 101, 181 (WW95)
- [142] Worthey, G., Faber, S. M. & Gonzalez, J. J. 1992, ApJ, 398, 69
- [143] Yamaguchi, R., Mizuno, N., Onishi, T., Mizuno, A., Fukui, Y. 2001, ApJ, 553, L185
- [144] Yoshii, Y., Tsujimoto, T., & Nomoto, K. 1996, ApJ, 462, 266
- [145] Yungelson, L. & Livio, M. 1998, ApJ, 497, 168
- [146] Zepf, S., E., & Silk, J. 1996, ApJ, 466, 114

FIG. 3: Age-metallicity relation for stars produced by the model. Note the large dispersion at early times.

FIG. 4: The metallicity distribution functions produced in clouds with four different initial mass functions as labeled.

FIG. 5: The sum of the MDFs for the four clouds shown in figure 4

FIG. 7: The abundances of the alpha elements when Fe yields are reduced by a factor of 2. Data is from Ryan et al. (1996) (triangles) and Norris et al. (2001) (circles). The small (dots) represent the model stars

FIG. 8: The abundances of the Fe-group elements, Mn, Ni, Cr, and Co . Data is from Ryan et al. (1996) (triangles) and Norris et al. (2001) (circles). The small (dots) represent the model stars

FIG. 9: The contribution from different progenitor masses to the value of  $[\text{Ca}/\text{Fe}]$ . The mass ranges are given in solar masses. The top left figure shows the whole range. Data is from Ryan et al. (1996) (triangles) and Norris et al. (2001) (circles). The small (dots) represent the model stars.

FIG. 10: The contribution from different progenitor masses to the value of  $[\text{Mg}/\text{Fe}]$ . The mass ranges are given in solar masses. The top left figure shows the whole range. Data is from Ryan et al. (1996) (triangles) and Norris et al. (2001) (circles). The small (dots) represent the model stars

FIG. 11: The contribution from different progenitor masses to the value of  $[\text{Si}/\text{Fe}]$ . The mass ranges are given in solar masses. The top left figure shows the whole range. Data is from Ryan et al. (1996) (triangles) and Norris et al. (2001) (circles). The small (dots) represent the model stars

FIG. 12: The contribution from different progenitor masses to the value of  $[\text{Ti}/\text{Fe}]$ . The mass ranges are given in solar masses. The top left figure shows the whole range. Data is from Ryan et al. (1996) (triangles) and Norris et al. (2001) (circles). The small (dots) represent the model stars

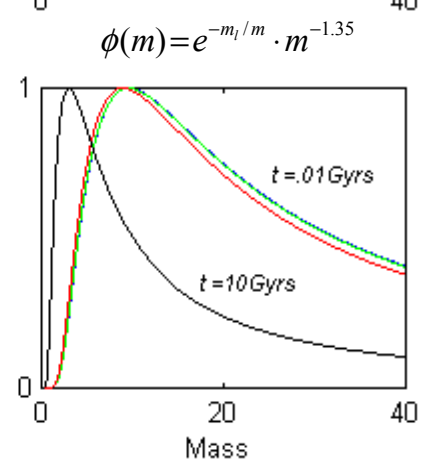
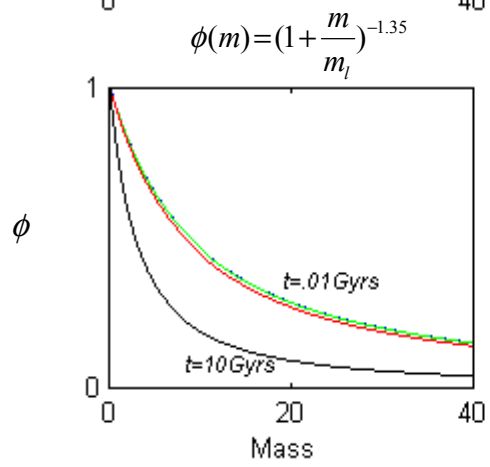
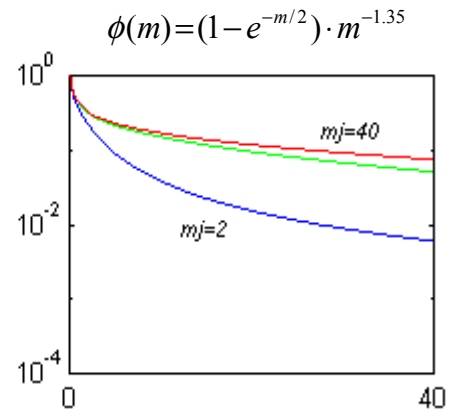
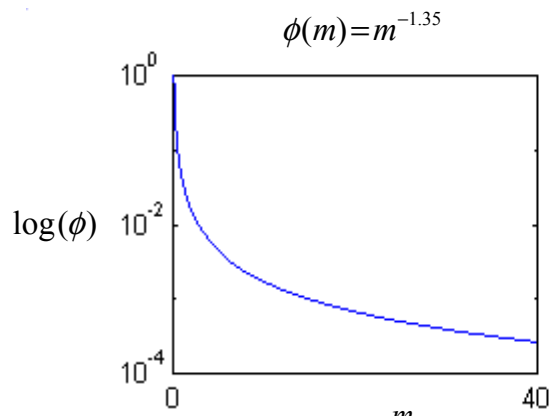
FIG. 13: The contribution from different progenitor masses to the value of  $[\text{Cr}/\text{Fe}]$ . The mass ranges are given in solar masses. The top left figure shows the whole range. Data is from Ryan et al. (1996) (triangles) and Norris et al. (2001) (circles). The small (dots) represent the model stars.

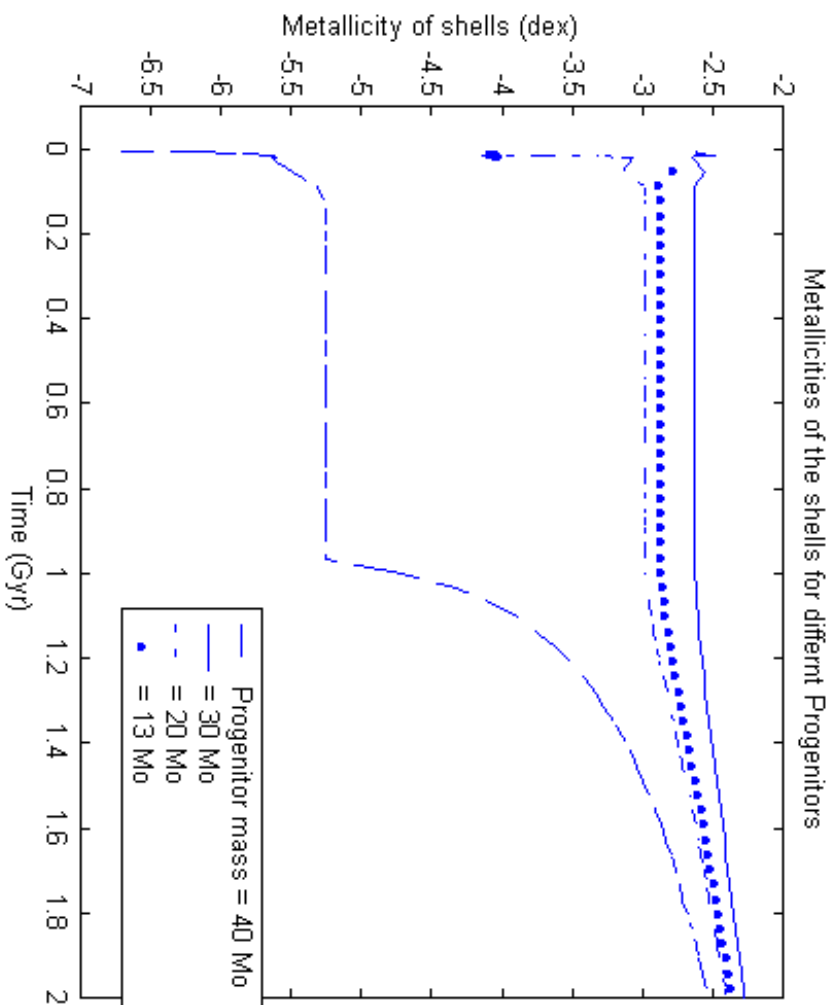
FIG. 14: The contribution from different progenitor masses to the value of  $[\text{Co}/\text{Fe}]$ . The mass ranges are given in solar masses. The top left figure shows the whole range. Data is from Ryan et al. (1996) (triangles) and Norris et al. (2001) (circles). The small (dots) represent the model stars

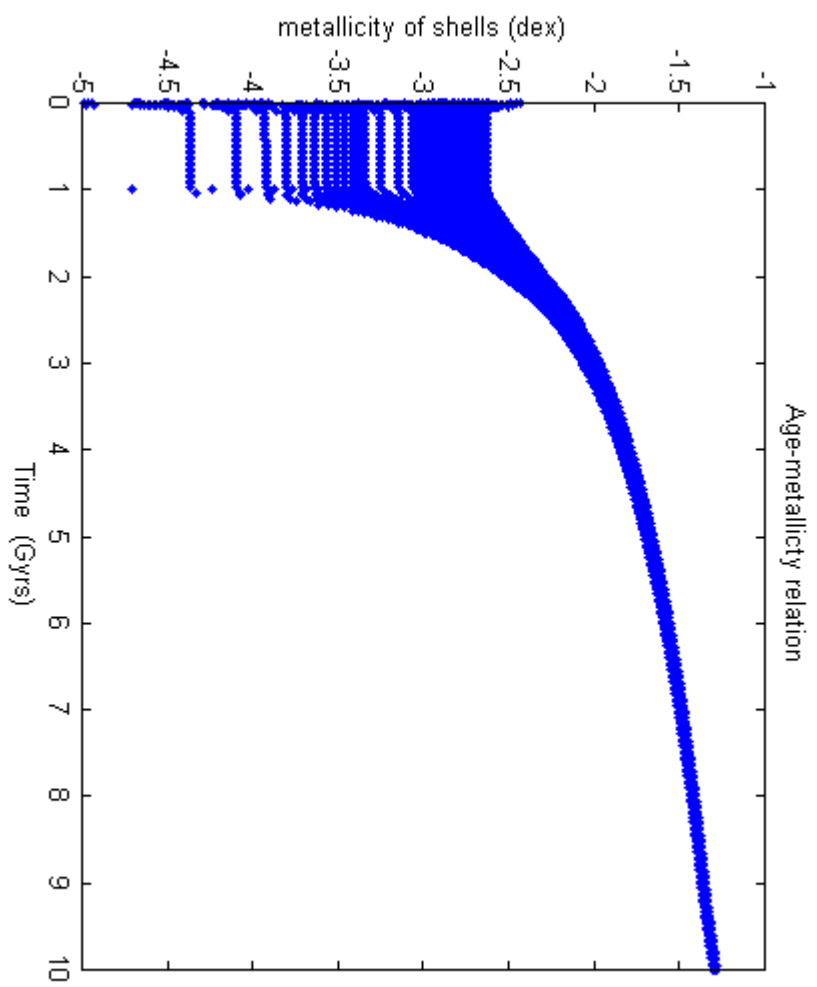
FIG. 15: The contribution from different progenitor masses to the value of  $[\text{Mn}/\text{Fe}]$ . The mass ranges are given in solar masses. The top left figure shows the whole range. Data is from Ryan et al. (1996) (triangles) and Norris et al. (2001) (circles). The small (dots) represent the model stars.

FIG. 16: The contribution from different progenitor masses to the value of  $[\text{Ni}/\text{Fe}]$ . The mass ranges are given in solar masses. The top left figure shows the whole range. Data is from Ryan et al. (1996) (triangles) and Norris et al. (2001) (circles). The small (dots) represent the model stars

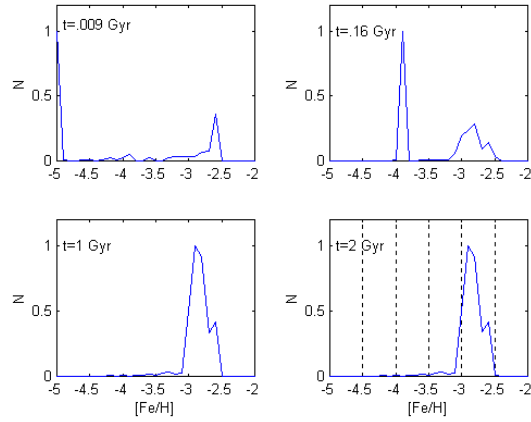
FIG. 6: The abundances of the alpha elements Mg, Ca, Si, and Ti. Data is from Ryan et al. (1996) (triangles) and Norris et al. (2001) (circles). The small (dots) represent the model stars



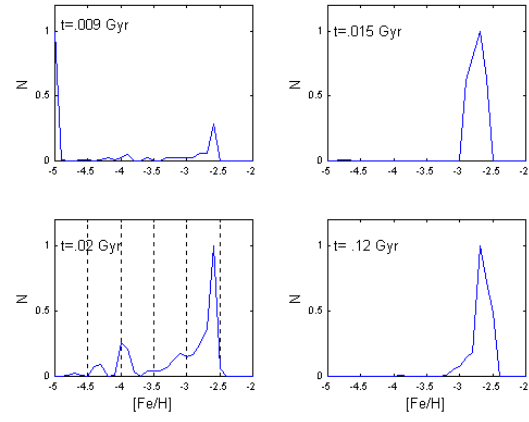




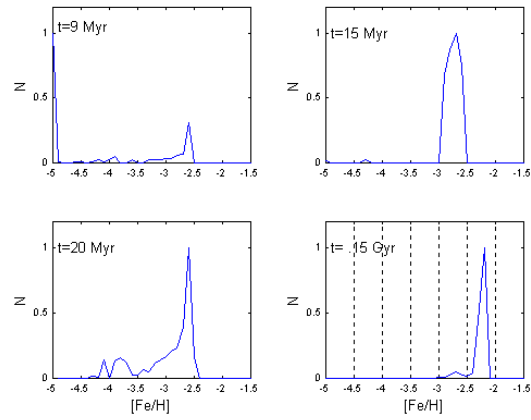
$$\Phi_1 = m^{-1.35}$$



$$\Phi_2 = m^{-1.35} (1 - e^{-m/m_j}), \quad m_j = 40$$



$$\Phi_3 = (1 + m/m_j)^{-1.35}$$



$$\Phi_4 = m^{-1.35} e^{-m/m_j}$$

